Science of Sintering, **49** (2017) 381-397

doi: https://doi.org/10.2298/SOS1704381T

UDK 621.926.087, 675.92.027, 692.533.1

Chemometric Analysis of Alternations in Coal Ash Quality Induced by Application of Different Mechano-chemical Processing Parameters

Anja Terzić[1*)], Lato Pezo[2], Ljubiša Andrić[3]
[1]Institute for Testing of Materials IMS, Vojvode Mišića Bl. 43, 11000 Belgrade, Serbia
[2]Institute of General and Physical Chemistry, University of Belgrade, Studentski Trg 12-16, 11000 Belgrade, Serbia
[3]Institute for Technology of Nuclear and other Raw Mineral Materials, Franchet d'Esperey 86, 11000 Belgrade, Serbia

Abstract:
The coal fly ash mechano-chemical activation conducted via high energy ultra-centrifugal mill was optimized using mathematical and statistical tools. The aim of the investigation was to accent the merits of alternations in ash processing schemes with a referral regarding the enhancement of the ash reactivity that will lead to its higher volume utilization as a cement replacement in concrete design. The impact of the processing parameters sets (number of rotor revolutions, current intensity, activation period, circumferential rotor speed, mill capacity) on the on the product's quality factors (grain size distribution, average grain size, micronization level, agglomeration tendency, specific surface area) was assessed via Response surface method, Standard score analysis and Principal component analysis in order to obtain the most favorable output. Developed models were able to meticulously predict quality parameters in an extensive range of processing parameters. The calculated r^2 values were in the range of 0.846-0.999. The optimal ash sample, that reached the Standard Score as high as 0.93, was produced using a set of processing parameters appropriate to experimental sequence with applied 120 μm sieve mesh. The microstructural characteristics were assessed using image-processing values and histogram plots of the activated fly ash SEM images.
Keywords: *High energy milling; Ultra-centrifugal activator; Analytical modeling; Electron microscopy; Construction composites.*

1. Introduction

The contemporary construction trade is confronted with problems regarding depleting and potential deficiency of natural resources, and imperiled environmental safely. For decades, concrete is the most commonly utilized building composite due to its strength, durability, resistance to atmospheric, chemical, and thermal impacts. Portland cement with its global fabrication rate of 3.6 billion metric tones per year is the base for concrete production [1]. Since cement production is prone to CO_2 emission, there is a huge risk of atmospheric pollution. Also, a task of sustainability has been imposed on the building industry, which means that cement and concrete fabrications have to become cost-effective, energy efficient,

*) **Corresponding author:** anja.terzic@institutims.rs

and to follow the green production regulations [1].

This can be achieved by alternations in used fuels, cement formulas and production, or by incorporation of waste raw materials into concrete blends [3, 4]. Various industrial byproducts and wastes that comply with strict environmental legislation are utilized as binding options for either total or partial cement substitutions: fly ash [5-8], silica fume [9, 10], blast furnace slag [11], recycled polymers [12, 13], sulfur [14, 15].

The application of green alternatives improves workability, durability and strength of the cementitious products, which is validated on both laboratory- and large-scale [16-21]. Fly ash is the most amply used byproduct because it offers cost-effectiveness and functionality; it meets engineering and architectural standards; the reserves are sufficient for long-term production; it is suitable for various applications - precast blocks, in-situ casting ready-mixes, shotcrete [18, 22-24].

The fly ash, as a result of coal combustion in power-plants, is fused in suspension and shifted by exhaust gases to the electrostatic precipitation zone where it solidifies into spherical glassy particles [25, 26]. The thusly obtained powder is a heterogeneous mixture of SiO_2, Al_2O_3, ferrous oxides (Fe_2O_3, Fe_3O_4) and CaO [27-30]. Due to pozzolanic behavior, the fly ash is used as an up to 30 % (usually 15–25%) cement substitution in concrete mix design. Fly ash contributes to the seven days concrete strength due to a chemical reaction with cement hydration products, and decreases permeability and initial heat evolution [30-36]. Pre-processing enhances the ash performances which initiates development of high-ash-share (50–60%) concretes [3, 4, 36-39]. The mechano-chemical activation promotes increased C_3S hydration, an early CH formation, a more compact structure, smaller pore size, lower porosity and higher compressive strength [36]. Mechanical milling is a solid-state powder processing technique that involves repeated particles welding and fracturing in a high-energy mill [30]. The ash reactivity is enhanced through the combined effects of decreased crystallite size and physicochemical changes induced in the bulk and on the surface without altering the overall chemistry of the material [3, 4, 17-19, 28, 36-39]. The sample is milled for the desired period based on the projected properties [3, 4]. The particles undergo severe plastic deformation as a consequence of mutual collisions and compression/shear forces acting between grinding media. The properties of milled powder are greatly affected by a number of process variables (mill type; grinding element type, size and quantity; milling time) [38, 39].

The optimization of the activation as a concrete synthesis pre-treatment is essential since the ultra-fine grinding is characterized by high energy consumption and low mill capacity. The experiment is based on multiple testing and inclusion of a mathematical method enables more efficient concluding [37]. Response surface methodology (RSM) is an effective tool for the treatment optimization and provision of systematic approach in determination of activation parameters influence [40-42]. The test variable interrelationships and their effect on the observed responses are described by RSM equations. The combined effect of the multiple process parameters (NRR, CI, MAP, CRS, Q) was observed during ultra-centrifugal activation of the ash via Retsch ZM-1 mill. The RSM technique determines the factor levels that generate the best product performance and it explores entire procedure with reduced number of experimental runs providing sufficient information for statistically valid results. The research purpose was to assess the ash quality based on the activation output (d_1/d_2, R_1/R_2, d', n, d_{95}, S_t, Sr) influenced by a different set of process parameters. The error variance, individual factors percentage contribution and the effect of the input factors significance are estimated via variance analysis (ANOVA). Comprehensive comparison between analyzed samples is achieved by Standard Score (SS), and samples are subsequently classified by Principal Component Analysis (PCA). The activated ash was characterized by scanning electron microscopy to understand the morphological changes upon milling. The aim of the study was to obtain an optimized ultra-centrifugal milling procedure and to produce micronized ash, which can be used as a value-added binder in concrete composites.

2. Experimental: materials and methods

The fly ash used in this investigation was fused in a lignite combustion chamber in a Serbian power-plant "Nikola Tesla" (TENT A) and collected directly from the filters. The ash sample was randomly taken and preserved in hermetically sealed boxes until further laboratory researches. The ash characterization in terms of chemical composition, mineralogy, crystallinity, surface chemistry and reactivity is of fundamental importance in the development of its various applications.

The chemical analysis (major, minor, and trace elements) was performed by X-ray fluorescence method on an XRF spectrophotometer ED 2000 (Oxford Instruments, UK) in accordance with the Standard: SRPS EN 196-2:2008. A representative sample of about 500 g was dried at 60°C prior to the testing. The obtained results were averaged. The fly ash international reference material obtained from the National Institute of Standards & Technology, USA, was applied in verification of the accuracy of the results of the analysis. The loss on ignition (LoI) was determined as a weight difference between two temperatures (20°C and 1000°C) with a delay of 4 h at maximal temperature. The results of the chemical analysis are given in Tab. I.

Tab. I Chemical composition of the fly ash.

Oxide, %	SiO_2	Al_2O_3	Fe_2O_3	TiO_2	CaO	MgO	P_2O_5	SO_3	Na_2O	K_2O	MnO	CO_2	LoI
	53.97	21.41	6.1	0.51	7.29	2.85	0.03	0.85	0.49	1.31	0.03	0.27	4.89

The fly ash contains organic and inorganic coal combustion residues, followed by trace hazardous contaminants (heavy metals, hydrocarbons, radioisotopes, dioxins) depending on the carbon origin and combustion conditions [41]. The organic fraction generally consists of unburned carbon (commonly expressed as LoI) and it might range from 2% to 90% [42]. The weight loss on ignition of the investigated ash sample was less than 5%. The inorganic fraction consists of predominantly siliceous and aluminous material (>75%). This ash fraction has a cementitious ability and acts as artificial pozzolana. According toASTMC618, the investigated fly ash belongs to the Class F. According to the X-ray diffraction analysis conducted on a Philips PW-1710 automated diffractometer using a Cu tube operated at 40 kV and 30 mA, major crystalline phases detected in the fly ash sample are quartz and mullite. Calcite, magnetite, hematite, fluorite, and anhydrite are traced in negligible amounts [41]. As specified by differential thermal analysis (Shimadzu, DTA-50) the ash contains moisture that evolves during heating. A peak at approximately 200°C corresponds to the volatilization of mechanically bonded H_2O molecule. Desorption of physically adsorbed and interlayer water molecules is completed at 450°C. The exothermic peak at approximately 500°C corresponds to the $CaCO_3$. The transition from β- to α-quartz takes place at 570°C [19, 41]. Fly ash contains grains sizing from several micrometers to 2 millimeters, however, only fine fractions are used in the experiment. The grain size distribution analysis obtained via cyclo-sizer (Warman International LTD, Australia) specified the mean grain diameter value as 0.148 mm. The fly grain-size distribution is shown in Fig. 1. The specific surface area of the initial ash sample determined by Brunauer–Emmett–Teller (BET) method was 281 m^2/kg. The bulk density of fly ash in loose condition (0.490 g/cm^3) was measured according to Archimedes' principle using a pycnometer and bulk density of pressed fly ash (0.715 g/cm^3) was measured using a column of liquid with a density gradient. The activated fly ash samples, coated with Au films for improvement of the conductivity prior to imaging, were analyzed by means of a JEOL JSM-5800 scanning electron microscope (JEOL, Japan). The Gwyddion software (http://gwyddion.net/) whose processing engine is based on the theory of implementation of the box-counting technique was used for microstructural characteristics assessing and calculations. The analysis was conducted on the SEM microphotographs of the activated ash samples.

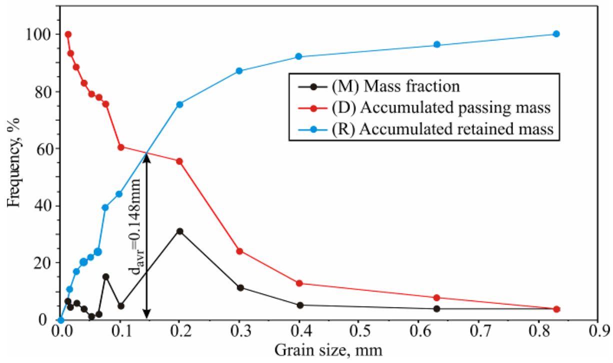

Fig.1. The grain-size distribution of the initial fly ash sample.

2.1. Mechano-chemical activation

A high speed rotor activator, i.e. an ultra centrifugal mill Retsch ZM-1 (Retsch GmbH, Germany) was used to achieve the improved reactivity of the ash particles. The ultra centrifugal activator was chosen for the experiment for its rapid and efficient size reduction capability. The ultra-centrifugal mill also consumes less energy than other activators (e.g. vibratory mill) [17-18, 38, 40]. The analytical fineness of the powder is achieved through repeated fracturing, cold welding and deformation of the particles. The mill's rotor hovers around the fixed ring sieve resulting in the movement of the ash particles which thusly undergo severe plastic deformation due to their mutual collision, and impact and shearing effects induced by grinding bodies. The sample initially passes through the hopper with splash-back protection onto the rotor, from where the centrifugal acceleration throws the treated material outward with vast huge energy. The ash is being pre-crushed during collision with wedge-shaped rotor teeth that move at a high pace, to be later micronized between the rotor and the ring sieve. The activator has 300 ml batch size, stainless steel grinding tools and set of sieves with trapezoid holes of 80, 120, 200 and 500 μm sizes. The adopted activation periods ranged from 3 to 30 min as it was established on the bases of previous researches and the values provided in the literature [3, 4, 17-18]. The achieved final fineness (median grain size) was generally less than 6 μm depending on the activation environment, i.e. adopted process parameters.

2.2. Statistical analyses

Obtained mechano-chemical activation results were expressed as average values for each experiment. The variance analysis (ANOVA) of the collected data was used to explore the consequences of the applied process variables. The PCA was used in the classification and differentiation of the samples acquired by the application of different process parameters. The observed samples were characterized and distinguished via Pattern recognition technique applied within results' descriptors. StatSoft Statistica 10.0® software was applied for assessing of RSM, ANOVA and PCA analyses of the acquired results [38-40]. The second order polynomial (SOP) model was fitted to the experimental data.

Nine responses (Y) and five process variables (X) were related to the nine models characterized by the form that is given in Eq. 1:

$$Y_k^l = \beta_{k0}^l + \sum_{i=1}^{2} \beta_{ki}^l \cdot X_i + \sum_{i=1}^{2} \beta_{kii}^l \cdot X_i^2 + \beta_{k12}^l \cdot X_1 \cdot X_2, \; k\text{=1-5}, \; l\text{=1-p}, \quad (1)$$

Where: β_{k0}^{l}, β_{ki}^{l}, β_{kii}^{l}, β_{k12}^{l} are constant regression coefficients; Y_k^l is d_1, d_2, R_1, R_2, d', n, d_{95}, S_t, or S_r; X_1 is NRR; X_2 is CI; X_3 is MAP; X_4 is CRS; and X_5 is Q.

In order to get a more complex insight in the ranking of observed samples, standard scores (SS) are evaluated using a chemometric approach on experimentally obtained d_1, d_2, R_1, R_2, d', n, d_{95}, S_t and S_r. Min-max normalization is one of the most commonly utilized methods for comparison of various characteristics of complex samples determined using multiple measurements, where samples are ranked based on the raw data ratio and extreme measurement values [38, 40]. The data units and scales of physical and chemical properties are different, therefore the data in each data set have to be transformed into normalized scores, dimensionless quantity derived by subtracting the minimum value from the raw data, and divided by the subtract of maximum and minimum value: $\overline{x}_i = 1 - \frac{\max_i x_i - x_i}{\max_i x_i - \min_i x_i}, \quad \forall i$ in case of "the higher, the better" criteria (used only for MAP score); and $\overline{x}_i = \frac{\max_i x_i - x_i}{\max_i x_i - \min_i x_i}, \quad \forall i$, in case of "the lower, the better" criteria, where x_i represents the raw data. The averaged sum of sample's normalized scores for different measurements gives a single unitless value (SS), which is a particular data combination obtained from different measuring methods with no unit limitation. Another set of samples can be easily employed in this elaboration in the future comparisons only by following this approach.

The objective of the conducted mathematical and statistical analyses was to optimize the mechano-chemical activation and to assess the quality of the activated ash for the given purpose and application.

3. Results and discussion

The bonding agent replacement materials with lower reactivity (i.e. pseudo pozzolana) in most cases are activated by cement during hydraulic reaction. Namely, during binding process the cement clinker acts as a catalyst and as a consequence the ash becomes very reactive in its presence. A mechanical activation of fly ash followed by standard activation by cement is able to provide significantly better performance of a concrete at all ages than that of untreated ash based material [17-19]. The major goal is to increase the ash share in the concrete composition up to 50-60% via mechanical pre-processing with no consequent deterioration of concrete performances. The optimization of the ash mechano-chemical activation is important as a justification of this method's application in the concrete production since the ultra-fine grinding is often regarded as an unsustainable and a high energy consuming procedure.

The properties of the micronized powders are affected by a number of process variables: type of activator, grinding bodies – quantity, material, size, type; initial sieve mesh size, number of rotor revolutions, current intensity, batch size of the vial, activation period, etc. The experiment was based on multiple testing and inclusion of mathematical methods for more efficient concluding. The first step in the investigation was to assess the benefits of ultra centrifugal Retsch ZM-1 mill utilization in the mechano-chemical activation of the fly ash. The applied process operation parameters (MAP, CRS, Q, SEC) and the obtained parameters of the activated products, such as mean grain diameter, theoretical/real specific surface area, specific consumption energy, characteristics of the grain size distribution, were mutually compared, estimated and evaluated. The activation procedure was conducted in four experimental sequences (MS80, MS120, MS200, and MS500) regarding applied initial sieves

(80, 120, 200 and 500 μm, respectively). The number of rotations per minute (NRR) was either 10.000 or 20.000 in each experimental sequence. The periods of activation (3-30 min) were founded on previous researches and the literature data [3,4,17,18]. The quality of the produced ash samples was assessed in terms of the following parameters: d_1, d_2, R_1, R_2, d', n d_{95}, S_t and S_r. The fly ash activation descriptive statistics data with optimal ranges are given in Tab. II.

The activation outcomes are divided into two groups: the first group characterizes the main properties of the activated product (d'; $d_{95,}$ S_t and S_r); and the second group defines the activation procedure efficiency with the obtained MAP and SEC values. The ideal theoretically accepted correlation occurs when the minimal d' value and the maximal S_t or S_r are assigned to the shortest activation period (MAP) and minimal energy consumption (SEC). The optimal ranges of the parameters have to be statistically processed and correlated, because the previously explained interrelation is rarely obtained either at experimental level or in the practice. As it can be seen in Tab. II which presents averaged results of the mechanical activation, the experimental sequence MS500 gave the shortest activation interval (MAP=8.8 min). Appropriately small amount of energy was necessary for this operation (223.8 kWh/t), however the obtained product parameters were inadequate in comparison with other experimental sequences: d' (4.5 μm) and S_t (389.8 m^2/kg). The displayed d' values for the MS120 and MS200 experimental sequences were: 3.6 μm and 4.0 μm, respectively. The used specific energy for the MS120 activation procedure was higher (SEC=260.3 kWh/t) than the energy spent during MS200 sequence (SEC=249.0 kWh/t). The MAP values applied in the MS120 and MS200 powder treatments were 14.3 min and 11.1 min, respectively. The calculated/measured values of specific surface area for these two sequences were: S_t/S_r^{MS120}=485.4/492.0 m^2/kg and S_t/S_r^{MS200}=440.9/446.3 m^2/kg. The processing duration of 17.5 min was registered for the MS500 experimental sequence, which was the longest MAP in the experiment. Also, the SEC (313.1 kWh/t) was comparatively higher than in other sequences. The MS80 activated ash with median grain size of 3.3 μm was smaller in comparison with mean diameters achieved in previously explained experimental sequences. Analogously, the specific surface area of the MS80 sample was high: S_t/S_r^{MS120}=518.2/528.5 m^2/kg. The MS80 sequence produced activated ash with excellent product related parameters; however the treatment parameters were unsustainable from the production point of view. Adversely, MS500 sequence was characterized by good production parameters, but inadequate characteristics of the activated product. The obtained average parameters values for the sequences MS120 and MS200 were comparably good for the concrete production; therefore these results were submitted to further statistical estimation.

Tab. II Descriptive statistics of activated fly ash samples.

	MS	CI	MAP	CRS	Q	SEC	d_1	d_2	R_1	R_2	d'	n	d_{95}	St	Sr
Min.		1.5	5.0	40.2	0.8	190.9	1.0	10.0	82.6	3.0	2.9	1.1	8.9	400.3	420.0
Max.		4.0	30.0	120.0	4.4	430.9	2.0	12.0	92.0	5.9	4.0	1.8	12.6	591.4	601.6
Ave.	80	2.8	17.5	82.1	2.3	313.1	1.5	10.8	87.3	4.5	3.3	1.3	10.4	518.2	528.5
SD		0.9	8.0	28.5	1.4	91.1	0.5	1.0	3.6	1.1	0.4	0.2	1.3	69.5	66.1
Var.		0.8	64.3	812.3	2.1	8300.4	0.3	1.1	13.0	1.2	0.2	0.0	1.8	4827.1	4363.3
Min. Opt.		-	-	-	-	-	-	-	-	-	3.0	1.2	7.5	400.0	400.0
Max. Opt.		-	-	-	-	-	-	-	-	-	3.3	1.3	8.0	500.0	500.0
Min.		1.4	5.0	41.5	0.8	185.2	2.0	10.0	84.0	2.8	3.1	1.2	9.3	415.0	422.1
Max.		3.9	25.0	119.2	4.4	410.2	3.0	15.0	92.8	5.0	4.5	1.9	15.0	583.4	591.3
Ave.	120	2.7	14.3	81.6	2.4	260.3	2.5	12.4	87.1	3.6	3.6	1.5	12.0	485.4	492.0
SD		0.9	6.6	27.6	1.4	82.7	0.5	2.2	2.8	0.7	0.5	0.2	2.2	61.0	62.1
Var.		0.8	43.9	762.0	1.9	6845.3	0.3	4.8	7.8	0.5	0.3	0.1	4.9	3724.5	3854.0
Min. Opt.		-	-	-	-	-	-	-	-	-	4.0	1.5	10.0	400.0	400.0
Max. Opt.		-	-	-	-	-	-	-	-	-	6.0	1.7	12.0	500.0	500.0
Min.	200	1.3	5.0	42.9	1.1	160.1	3.0	12.0	84.0	3.9	3.3	1.3	10.8	380.2	386.0

Max.		3.6	20.0	120.7	4.9	395.9	4.0	16.0	88.9	5.9	4.9	1.9	15.6	507.2	514.2
Ave.		2.5	11.1	82.6	2.5	249.0	3.4	13.4	86.5	4.6	4.0	1.5	12.7	440.9	446.3
SD		0.8	5.1	28.2	1.4	77.2	0.5	1.5	1.7	0.7	0.6	0.2	1.7	44.4	44.6
Var.		0.7	26.1	797.6	1.9	5955.2	0.3	2.3	2.8	0.5	0.4	0.1	2.9	1967.9	1989.5
Min. Opt.		-	-	-	-	-	-	-	-	-	6.0	1.1	14.0	400.0	400.0
Max. Opt.		-	-	-	-	-	-	-	-	-	8.0	1.3	17.0	500.0	500.0
Min.		1.3	3.0	43.2	1.1	150.3	3.0	12.0	89.5	3.2	3.5	1.3	11.3	305.8	306.0
Max.		3.3	17.0	119.8	4.8	360.9	5.0	17.0	94.3	5.3	5.4	1.9	16.3	495.5	499.0
Ave.	500	2.3	8.8	82.1	2.6	223.8	4.0	14.6	91.5	4.2	4.5	1.5	14.1	398.8	402.0
SD		0.8	4.8	28.2	1.3	69.8	0.8	1.8	1.9	0.7	0.7	0.2	1.9	64.1	64.7
Var.		0.6	23.1	796.2	1.7	4877.2	0.6	3.4	3.5	0.5	0.4	0.0	3.7	4107.0	4189.6
Min. Opt.		-	-	-	-	-	-	-	-	-	10.0	1.4	19.0	400.0	400.0
Max. Opt.		-	-	-	-	-	-	-	-	-	12.0	1.6	24.0	500.0	500.0

3.1. Principal component analyses

The PCA was employed for the reduction of the variables' quantity and for the detection of interrelations among experimentally obtained parameters and factors of various processing treatments applied to different ash samples. The full auto scaled data matrix was submitted to the PCA. Data trends were visualized and the descriptors' discriminating efficiency was obtained from the scatter plot of samples using the first two principal components (PCs) issued from PCA of the data matrix. The PCA score plot is illustrated in Fig. 2.

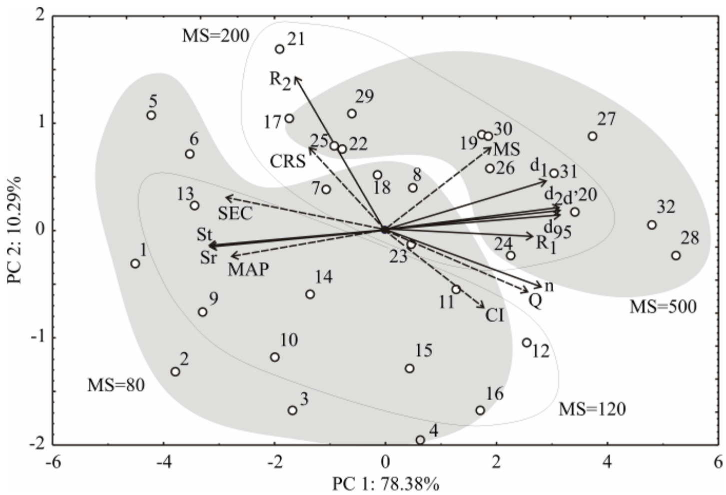

Fig. 2. PCA biplot for characteristics of fly ash.

The analysis gave a precise differentiation of the observed samples. Activated ash samples produced in MS80 and MS120 experimental sequences are located at the bottom of the diagram. The MS80 is positioned on the left of the PCA graph and MS120 is on the right. The set of results of these two experimental sequences is mutually intersected and characterized by the highest S_t and S_r values. The samples produced in MS500 experimental sequence are located at the right side and towards the upper right corner of the graphic, having the greatest d_2, R_1, R_2, d', and d_{95} values. The set of results belonging to the MS200 experimental sequence is located partially at the center of the PCA graphic and partially on the left side transecting the MS500 group of results. The results of the descriptive statistics, i.e. PCA score plot, and the table of optimal ranges (Tab. II) are in agreement regarding the MS80 being the experimental sequence with the highest obtained specific surface areas: S_t and S_r. However, at the same time, the MS80 is not the most optimal solution, because this sequence is characterized by the longest activation period and the greatest amount of consumed energy for the activation process (SEC). An opposite correlation occurred during

MS500 experimental sequence: d' is high and S_t/S_r is low, while MAP is short. Namely, both interrelations are economically unsustainable, because they either require too much energy for the treatment, or produce materials with inadequate properties.

Quality results show that the first two principal components, accounting for 88.67% of the total variability can be considered sufficient for data representation. d_1 (which contributed 11.1% of total variance, based on correlations), d_2 (13.0%), d' (13.2%), n (10.5%), d_{95} (13.2%), S_t (12.9%) and S_r (13.0%) were found the most influential for the first factor coordinate calculation, while the contribution of R_2 (76.4%) and n (10.1%) were the most important variables for the second factor coordinate calculation.

3.2. Response Surface Methodology

The analysis of variance - ANOVA showed significant influence of the independent variables to the responses and interactions of these variables. Also, it was indicated which of responses were significantly affected by varying activation process combinations (Tab. III).

It was observed that the SOP models for all variables were statistically significant and the response surfaces were fitted to the models. The calculation of R_1 was mostly influenced by the quadratic terms of MS and CI (statistically significant at $p<0.10$ level). The d' calculation was affected by linear terms of MAP, CRS and Q in SOP model, statistically significant at $p<0.05$ level. Also, the calculation of d' was influenced by the quadratic terms of CRS ($p<0.01$) and Q ($p<0.05$), and by non-linear terms of NRR×MAP, NRR×CRS and MAP×CRS (statistically significant at $p<0.01$ level) and MAP×Q ($p<0.05$ level). The computations of St and S_r were influenced by the linear terms of CI and Q ($p<0.01$) and also MAP ($p<0.05$), the quadratic terms of Q ($p<0.01$) and MAP ($p<0.05$). These parameters are also influenced by non-linear term MAP×Q (statistically significant at $p<0.01$ level). The interrelations with MS parameter are expected since d_1 and d_2 values are acquired from the grain-size distribution graph of the activated ash; the R_1 and R_2 represent accumulated retained masses that correspond to the d_1 and d_2; and d', d_{95}, and S_t originate from the grinding kinetic model (Rosin-Rammler-Sperling equation) which makes them dependent on the grain size distribution of the activated sample [18, 40]. The SOP model proved that parameters of the activation procedure (e.g. mill's capacity, circumferential rate of the rotor) and their correlations with MAP or NRR particularly determine the output data.

The results that are provided in the Tab. III show values of the residual variance and determination coefficient (r^2). The residual variance represents an absence of fit variation that illustrates various contributions except for the higher order terms and shows that the model failed to represent the data in the experimental domain at which points were not included in the regression [40]. The r^2 coefficient is the ratio of the residual variation to the total variation explained by its magnitude, as well as the variability proportion in the response variable, which is accounted for the regression analysis [40]. All SOP models showed negligible lack of fit tests, which means that these models are acceptable for data representation. The r^2 values are high (d_1 (0.988), d_2 (0.959), R_1 (0.980), R_2 (0.846), d' (0.999), n (0.983), d_{95} (0.971), St (0.998), and S_r (0.997)) and they show the adequate fit of the proposed model to the experimental results. High accuracy of the obtained d', d95, and St parameters are explained by adequate choice of d_1 and d_2 values on the ash grain-size distribution diagram which approves the application of the RRS equation [40].

Since descriptive statistics and the PCA highlighted the MS120 experimental sequence as the ash mechano-chemical pre-treatment with the most adequate results, 3D diagrams for the most important response parameters are plotted in order to visualize the obtained outcome and to observe fitting of regression models to experimental data (Fig. 3).

Tab. III The analysis of variance of activated fly ash parameters.

	df	d_1	d_2	R_1	R_2	d'	n	d_{95}	St	Sr
NRR	1	0.204	0.442	0.069	0.359	0.016	0.008	0.002	2.5	9.7
MS	1	0.076	0.031	4.156	0.149	0.007	0.002	0.012	18.7	60.5
MS^2	1	0.083	0.467	6.395^{**}	0.095	0.002	0.003	0.011	192.6	350.2
CI	1	0.071	0.147	0.043	0.179	0.022	0.000	0.007	1883.7^{+}	1893.2^{+}
CI^2	1	0.005	0.235	6.357^{**}	0.338	0.001	0.004	0.265	76.3	18.3
MAP	1	0.080	0.105	3.627	0.189	0.038^{*}	0.000	0.208	665.7^{*}	654.5^{*}
MAP^2	1	0.089	0.475	2.730	0.120	0.007	0.000	0.630	809.7^{*}	661.1^{*}
CRS	1	0.249	0.594	0.111	0.183	0.041^{*}	0.008	0.016	234.2	178.5
CRS^2	1	0.047	0.041	0.145	0.059	0.105^{+}	0.006	0.001	41.5	54.8
Q	1	0.031	0.127	0.317	0.017	0.059^{*}	0.001	0.047	2085.6^{+}	1920.8^{+}
Q^2	1	0.000	1.233	3.158	0.090	0.047^{*}	0.011	0.610	1861.7^{+}	1302.4^{*}
NRR × MS	1	0.002	0.368	4.985	0.304	0.000	0.003	0.235	0.2	15.1
NRR × CI	1	0.001	0.181	4.655	0.296	0.002	0.001	0.244	44.4	9.2
NRR × MAP	1	0.229	0.129	0.046	0.069	0.073^{+}	0.005	0.012	84.9	92.2
NRR × CRS	1	0.052	0.034	0.615	0.096	0.098^{+}	0.005	0.017	49.1	69.2
NRR × Q	1	0.000	0.110	4.428	0.147	0.014	0.006	0.302	139.8	66.3
MS × CI	1	0.010	0.179	4.808	0.246	0.002	0.003	0.105	40.4	108.0
MS × MAP	1	0.131	0.005	3.850	0.101	0.019	0.001	0.006	19.4	50.8
MS × CRS	1	0.013	0.780	3.700	0.333	0.001	0.003	0.487	73.4	16.2
MS × Q	1	0.036	0.045	4.369	0.184	0.004	0.003	0.027	67.6	134.2
CI × MAP	1	0.165	0.001	1.393	0.029	0.009	0.000	0.058	475.0^{**}	357.7
CI × CRS	1	0.000	0.129	3.859	0.336	0.010	0.000	0.184	0.7	4.2
CI × Q	1	0.018	0.254	6.094	0.192	0.017	0.008	0.284	352.2^{**}	188.2
MAP × CRS	1	0.262	0.318	0.101	0.042	0.083^{+}	0.006	0.008	344.9^{**}	317.6
MAP × Q	1	0.050	0.829	0.132	0.001	0.048^{*}	0.004	0.474	2173.9^{+}	1752.3^{+}
CRS × Q	1	0.002	0.005	3.941	0.144	0.008	0.003	0.161	2.3	0.6
Error	5	0.474	6.020	6.388	3.621	0.020	0.028	4.356	413.3	487.0
r^2		0.988	0.959	0.980	0.846	0.999	0.983	0.971	0.998	0.997

$^{+}$Significant at $p<0.01$ level, *Significant at $p<0.05$ level, **Significant at $p<0.10$ level, 95% confidence limit, error terms have been found statistically insignificant

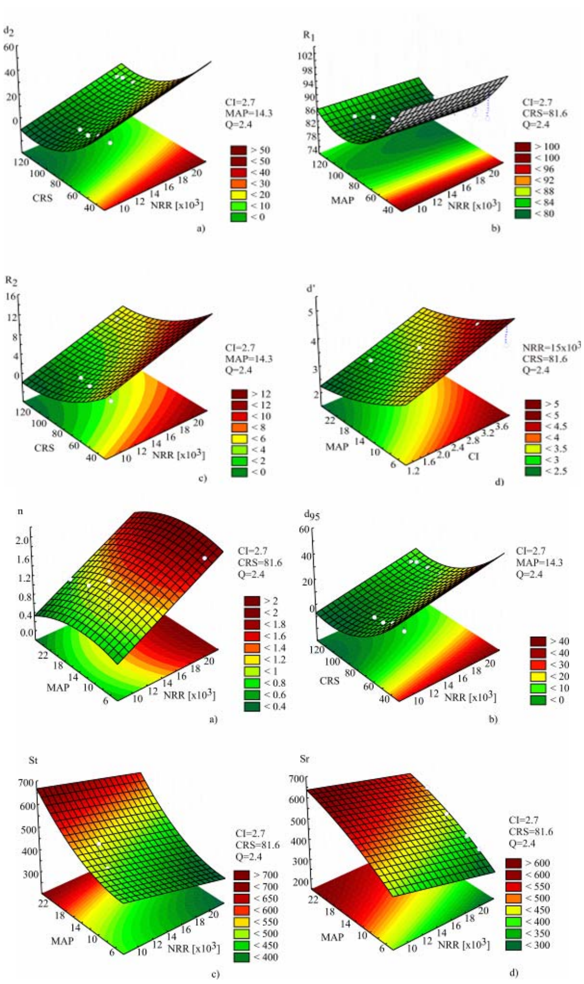

Fig. 3. Visualization of the most important response parameters determined by SOP.

3.4. Standard score analysis

The SS is a unitless value that is in consistent accordance with scrutinized assays (d', n, d_{95}, S_t and S_r). Namely, it is a mean value of standard score transformed from the initial data obtained through different analyses in which every singular item was computed assigning each applied parameter the equal weight. SS illustrates the precise rank of ash samples, even though it is a relative index and may not represent a specific characteristic of a sample. The SS with values that are above 0.700 characterize the high standard in ash properties. The SS analysis of experimental measurements showed optimal processing parameters (Tab. IV). Utilization of the standard score analysis and displaying the SS of differently processed ash samples can be referenced for developing strategies for improving composite materials based on industrial by-products.

Tab. IV Standard score analysis of ash processing parameters.

No.	MS	CI	MAP	CRS	Q	SEC	d_1	d_2	R_1	R_2	d'	n	d_{95}	S_t	S_r	SS
1	80	2.8	20	55	2.363	360.65	2	10	88.9	3.18	3.2	1.39	9.76	500.2	512.79	0.86
2	120	3.35	8	99.5	2.678	275.2	3	13	86.0	2.9	3.87	1.5	12.65	447.2	450.45	0.93
3	200	2.65	10	56	3.232	180.37	4	15	88.4	4.5	4.6	1.5	14.3	430.58	440	0.83
4	500	1.7	12	64	1.985	190.27	4	15	90.1	4.1	4.75	1.42	14.55	445.2	448	0.723

The optimal sample was obtained using No. 2 (MS120) set of processing parameters (obtained SS was equal to 0.93), which is in accordance with previously presented results (descriptive statistics, PCA). Another set of parameters, No. 1, 3 and 4 (MS80, MS200 and MS500) gave lower SS, between 0.723 and 0.86. Therefore, the MS120 experimental sequence can be adopted as an optimal set of activation parameters since d', d_{95}, S_t, S_r, and also SEC and MAP values are recognized as satisfactory. This mechano-chemical treatment can be regarded as energetically sustainable and cost-effective. Namely, according to the SS analysis, the MS120 activation procedure characterized by short MAP (8 min) and relatively low SEC (275.2 kWh/t) produced ash raw material with a mean diameter of 3.87 μm and specific surface area of 450.45 m^2/kg. Besides reduction of the negative effect of ash samples inherent properties on the final score, the application of this pre-treatment will increase the ash-cement replacement factor and improve the characteristics of the final product.

3.5. Microstructural analysis

The SEM microphotographs of the fly ash samples produced via MS80, MS120, MS200 and MS500 activation set of parameters are given in Fig. 4 (a, b, c, and d).

The applied pre-processing improved ash reactivity through changes that are recorded in the microphotographs – the alternations in the grain size and shape, as well as the changes in the physic-chemical properties that initiated further modifications in both bulk and on the surface (phase transformations, structural defects multiplication, rearrangements in microstructure, surface modifications) [4]. The application of different processing parameters of the same high-energy mill gave different results, i.e. variations in amounts of reactive fine fraction and glass content. According to the chemical composition (Tab. I), the ash contained inorganic non-combustible substance characterized by considerable amounts of SiO_2, Al_2O_3, CaO, Fe_2O_3 and minor amounts of K_2O, Na_2O, P_2O_5, MgO and TiO_2. The starting powder consisted of mostly spherical grains (solid and hollow spheres) and smaller amount of irregularly shaped grains, with a wide range size distribution (0.013-0.830 mm). The spherical grains had either smooth glassy surface or increased superficial porosity. Also, a certain amount of unburnt coal which is extremely porous was present [17-19, 41]. The harsh impact and shear forces acting on the ash grains during mechano-chemical activation resulted in an increased percent of fractured particles with irregular shapes and rough surface textures, even though the spherical grain remains as the most abundant particle shape in the activated mixture (Fig. 4). During high-energy milling, the minimal achievable grain size is usually limited by agglomeration process or a particles' compaction. Namely, smaller particles adhere to the surface of the larger spheres creating one larger grain due to the inter-particle forces. The SEM analysis conducted upon activation of ash samples revealed mentioned size, shape and morphology changes that are in direct relation with the varieties in the treatment's parameters.

The MS80 set of parameters (Fig. 4a) produced the ash mixture with the smallest median grain diameter according to the statistical analysis. The highest amount of small, irregularly shaped grains with torn edges is present in this activated ash mixture. Also, large solid particles without prominent superficial porosity, which appeared as a result of compaction of smaller grains due to longer milling, are visible in the microphotograph. This experimental sequence is also characterized by significant participation of agglomerations made of smaller grains that probably have calcite origin [34]. An ash mixture with slightly larger grains but with significantly less agglomerations and a higher percentage of regular shapes was produced applying the MS120 set of parameters (Fig. 4b). Only one large porous irregularly shaped grain that might correspond to a $CaCO_3$ agglomeration is recorded in the microphotograph. Specific mullite crystals in the shape of small needles that have the microstructural reinforcing ability and angular (hexagonal) quartz particles [35] are present in the mixture. Majority of grains exhibits a superficial porosity in the form of scattered small circular voids. A microphotograph Fig.4c shows that the MS200 produced ash mixture with comparatively larger mean grain-diameters than two previous experimental sequences, which is in accordance with statistical analysis. Most of the grains in the mixture are spherical (aluminosilicate minerals), although irregularly shaped grains (quartz and mullite) are present, too. Pseudospheres and cenospheres (spherical grains composed of various layers or grains) that usually correspond to the presence of magnetite [4, 41] are noticed. Such grains can increase water absorption of a composite since they are intersected by pore channels and therefore have increased internal porosity. The MS500 set of parameters (Fig. 4d) produced the ash mixture that consists of relatively large grains mostly in form of approximate spheres with numerous pores on the surface, even though other irregular grain shapes are present, too. This experimental sequence was excluded from the observation due to the low SS value (0.723). The difference in mean grain diameter of MS120 and MS200 was accounted for only 10%; however the Standard Score analysis highlighted the MS120 set of parameters as the option with the highest SS. The average grain size of the MS120 sequence is only 9% larger than that of MS80 sequence, but having in mind extended MAP and higher SEC of MS80, the ash produced by MS120 set of parameters should be considered as the optimal outcome.

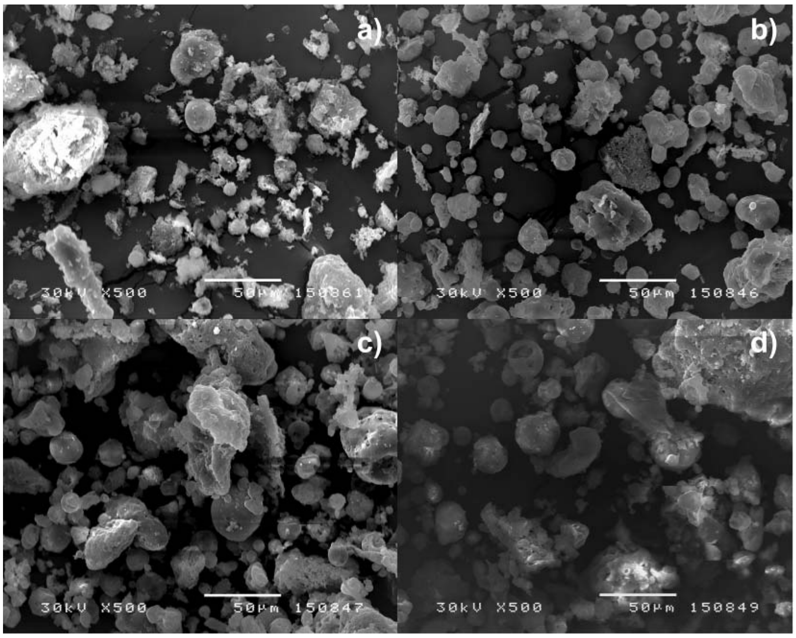

Fig. 4. SEM of activated ash produced via: a) MS80; b) MS120; c) MS200; d) MS500.

The microstructural image analysis was conducted in order to depict the complexity of the ash microstructure and to estimate the geometry of the grains and morphology of their surfaces. The calculation was performed via Gwyddion software (http://gwyddion.net/) using the SEM microphotographs as a source material for the program. The microstructural characteristics are estimated on the basis of the histogram plots of various SEM images of activated fly ash samples (Fig. 4a-d) and thusly extracted image-processing values. The SEM microphotograph represents a micro-surface in gray tones therefore it can be used for relatively accurate reconstruction of the real surface due to the topological equivalence of the real surface and its microphotograph. Namely, there are three types of surfaces: real surface; the photo of the surface (SEM); and 3D reconstruction of the surface as given in Fig. 4. The goal is to find approximate but accurate enough topography of the real surface, i.e. fly ash grain.

The Fig. 5a-d illustrates "density" and morphology of the observed specimens. The sample obtained via MS120 set of parameters (Fig. 5b) contains higher amount of spherical grains of rather uniform size. The sample MS80 (Fig. 5a) shows certain level of disorder in size uniformity, i.e. the alternations in grain sizes, from very small grains sizing less than 3 μm to huge particle's agglomerations, are evident. The 3D reconstructions of MS200 and MS500 (Fig. 5c and d) samples showed proportionally higher grain-sizes than MS120.

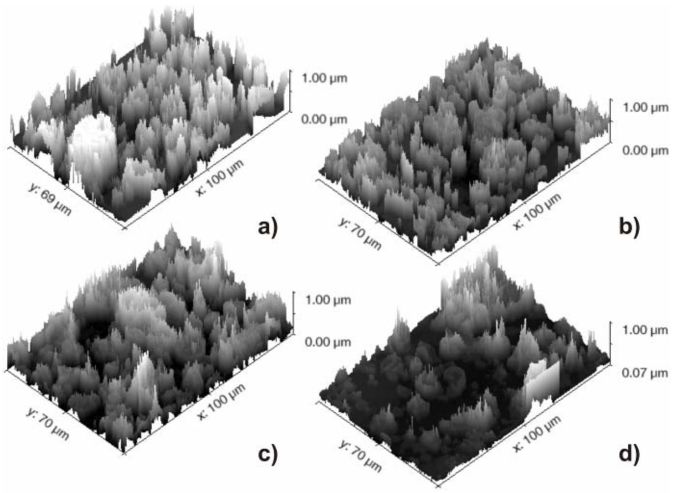

Fig. 5. Numerically generated surface plots from microphotographs given in the Fig. 4.a-d.

After extracting 3D data from the gray-level SEM, a numerically generated surface with peaks at white spots and valleys at dark parts is used in the construction of the 2D diagrams. Thusly obtained analyses of data variance of the SEM picture columns and rows are given in Fig. 6.

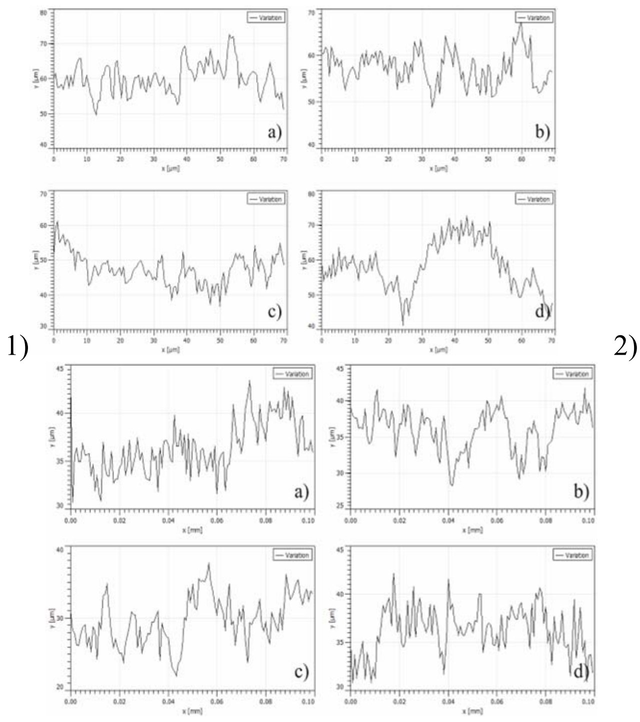

Fig. 6. The analysis of variance of SEM picture: 1) columns and 2) rows.

The diagram that shows typical, large number of peaks is giving an impression of the random distribution which is a firm confirmation of the complex topography of the numerical surfaces given in Figure 6a-d. The samples produced with MS500 and MS80 set of parameters show the weakest uniformity in grain size distribution. The SEM analysis also highlighted agglomerations pronounced agglomeration tendency as a characteristic of these two experimental sequences. The MS500 sample was also excluded by statistical analysis due to the low SS value. The MS120 experimental sequence can be adopted as the optimal activation treatment because it produced the ash mixture that consisted of relatively smooth grains, with rather uniform grain size distribution and the minimal percentage of present agglomerations which is in consistency with statistically determined results.

4. Conclusion

The cement replacement material production technology that deploys mechano-chemical activation and its transferal into an economically attractive and sustainable solution for the design of fly ash based composites is highlighted. The assets of different ash processing schemes are emphasized, and a specific attention was paid on enhancing of the ash reactivity to achieve its high volume utilization in concrete design. The main purpose of the investigation was to optimize the ash activation via ultra-centrifugal mill using mathematical and statistical tools. The application of the RSM method enabled significant reduction of number of experimental runs, but provided sufficient information for the statistically valid results. The position of quality data and the directions for the improving of the treated ash characteristics was achieved via PCA application and the disclosing of the different ash samples coordinates. A multiple influence of linear and nonlinear terms of second order polynomial model was exhibited by ANOVA calculation of the response parameters. SS analysis promoted the optimal output basing on the evaluation of multiple influences of the parameters, which altered during technological treatment, on the micronized ash quality. The microstructural computer analysis helped in assessing of the samples' surfaces topography and depicted the complexity of the ash microstructure.

The statistically recommended set of processing parameters that produced the activated ash with optimal characteristics: MS=120 μm, CI=3.35 A, MAP=8 min, CRS=99.5 m/s, SEC=275.2 kWh/t and Q=2.678 kg/h. The quality of thusly obtained product is described with following response variables: d_1=3 μm, d_2=13 μm, R_1=86 %, R_2=2.9 %, d'=1.5 μm, n= 0.6, d_{95}=12.65 μm, S_t=447.2 m^2/kg and S_r=450.45. Other analyzed sets of processing parameters showed either high SEC (e.g. MS80) which is considered energetically and economically infeasible, or produced inadequate response values and low SS (e.g. MS500 and MS200). Statistical tools highlighted the MS120 combination of activating parameters as a means for production of optimal ash sample that is characterized by relatively uniform grain sizes, rather compact grain structure, small pores, low porosity, and vague agglomeration tendency. The results of the microstructural computer analysis were in consistency with statistically determined results and SEM analysis by revealing the MS120 ash as uniform grain mixture with smooth grain surfaces. It was demonstrated that the mechano-chemical activation achieved via high energy mill may greatly enhance the fly ash characteristics and reactivity, which turns a waste disposal problem into a cost-effective opportunity for reducing an environmental burden, opens new possibilities for the ash industrial application and efficiently contributes to rationalization of cementitious composites production technology.

5. Nomenclature

MS	sieve mesh size, μm
NRR	number of rotor revolutions, rotations per minute / rpm

CI	current intensity, A
MAP	mechano-chemical activation period, min
CRS	circumferential rotor speed, m/s
Q	capacity, i.e. batch size of ultra-centrifugal mill, kg/h
SEC	specific consumption energy (engine power/mill capacity), kWh/t
d_1, d_2	mesh sizes of the used sieves, μm
R_1, R_2	accumulated retained mass, %
d'	average grain size, μm
d_{95}	sieve mesh size appropriate to 95 % accumulative passing mass of the ash, μm
n	level of micronization
S_t	calculated (theoretical) specific surface area, m^2/kg
S_r	real specific surface area, m^2/kg

6. Acknowledgements

This investigation was supported by Serbian Ministry of Education, Science and Technological Development and it was conducted under projects: ON 172057, III 45008, TR 31055 and TR 34006. The authors would like to express mutual gratitude to colleagues from the Faculty of Electronic Engineering in Niš for performing the SEM analysis.

7. References

1. M. Imbabi, C. Carrigan, S. McKenna, International Journal of Sustainable Built Environment, 1 (2012) 194.
2. www.iea.org/publications/freepublications/publication/Cement.pdf
3. F. Zhao, W. Ni, H. Wang, H. Liu, Resources Conservation & Recycling, 52 (2007) 303.
4. R. Kumar, S. Kumar, S. Mehrotra, Resources Conservation & Recycling, 52 (2007) 157.
5. R. Ibrahim, R. Hamid, M. Taha, Construction and Building Materials, 36 (2012) 779.
6. M. Ashtiani, A. Scott, R. Dhakal, Construction and Building Materials, 47 (2013) 1217.
7. F. Okoye, J. Durgaprasad, N. Singh, Ceramics International, 42 (2016) 3000.
8. T. Xie, T. Ozbakkaloglu, Ceramics International, 41 (2015) 5945.
9. M. Nili, A. Ehsani, Materials & Design, 75 (2015) 174.
10. E. Ahmed, B. Khalil, M. Anwar, Water Science, 29 (2015) 36.
11. X. Huang, Z. Wang, Y. Liu, W. Hu, Construction and Building Materials, 112 (2016) 241.
12. M. Dalhat, H. Wahhab, Construction and Building Materials, 119 (2016) 206.
13. T. Gupta, R. Sharma, S. Chaudhary, International Journal Of Impact Engineering, 83 (2015) 76.
14. C. Yang, X. Lv, X. Tian, Y. Wang, S. Komarneni, Construction and Building Materials, 73 (2014) 305.
15. M. Shin, K. Kim, S. Gwon, S. Cha, Construction and Building Materials, 69 (2014) 167.
16. N. Kockal, T. Ozturan, Journal of Hazardous Materials 179 (2010) 954.
17. A. Terzić, L. Pezo, V. Mitić, Z.Radojević, Ceramics International, 41 (2015) 2714.
18. A. Terzić, Lj. Andrić, V. Mitić, Ceramics International, 40 (2014) 12055.

19. A. Terzić, N. Obradović, Lj. Andrić, J. Stojanović, V. Pavlović, Journal of Thermal Analysis and Calorimetry,119 (2015) 1339.
20. M. Rafieizonooz, J. Mirza, M. Salim, M. Hussin, E. Khankhaje, Construction and Building Materials, 116 (2016) 15.
21. http://www.ecoba.com/ecobaccpexs.html, European Coal Combustion Products Association e.V.
22. H. El-Didamony, E. El-Rahman, R. Osman, Ceramics International, 38 (2012) 201.
23. A. Pereira, J. Akasaki, J. Melges, M. Tashima, L. Soriano, M. Borrachero, J. Monzó, J. Payá, Ceramics International, 41 (2015) 13012.
24. S. Riahi, A. Nazari, Ceramics International, 38 (2012) 4467.
25. I. Acar, M. Atalay, Fuel, 106 (2013) 195.
26. A. Patil, A.Shanmugharaj, S. Anandhana, Powder Technology, 272 (2015) 241.
27. E. Soco, J. Kalembkiewicz, Journal of Hazardous Materials, 145 (2007) 482.
28. M. Izquierdo, O. Font, Journal of Hazardous Materials, 181 (2010) 82.
29. M. Gesoglu, E. Guneyisi, T. Ozturan, H. Oznur, D. Asaad, Composites Part B-Engineering, 60 (2014) 757.
30. S. Kumar, R. Kumar, Ceramics International, 37 (2011) 533.
31. Z. Xie, Y. Xi, Cement and Concrete Research, 31 (2001) 1245.
32. W. Bing-wen, H. Yun-bing, Z. Fan, Y. Lei, Z. Jie, Procedia Earth and Planetary Science, 1 (2009) 736.
33. S. Sinthaworn, P. Nimityongskul, Waste Management, 29 (2009) 1526.
34. M. Sadique, H. Al-Nageim, W. Atherton, L. Seton, N. Dempster, Construction and Building Materials, 43 (2013) 480.
35. A. G. Patil, S. Anandhan, Powder Technology, 281 (2015) 151.
36. P. Stellacci, L. Liberti, M. Notarnicola, P. Bishop, Chemical Engineering Journal, 149 (2009) 11.
37. P. Stellacci, L. Liberti, M. Notarnicola, P. Bishop, Chemical Engineering Journal, 149 (2009) 19.
38. A. Terzić, L. Pezo, V. Mitić, Ceramics International, 42 (2016) 6301.
39. U. Ulusoy, Powder Technology, 188 (2008) 133.
40. A. Terzić, L. Pezo, Lj. Andrić, Ceramics International, 41 (2015) 8894.
41. A. Terzić, Lj. Miličić, International Journal of Coal Preparation and Utilization, 33 (2013)1 59.
42. H. Y. Leung, J. Kim, A. Nadeem, Jayaprakash Jaganathan, M. P. Anwar, Construction and Building Materials, 113 (2016) 369.

Садржај: *Механо-хемијска активација угљеног летећег пепела спроведена помоћу високоенергетског центрифугалног млина је оптимизована математичким и статистичким алаткама. Циљ истраживања је био да се нагласи значај алтернација у процесним шемама активације пепела који за крајњи исход има повећање рекативности пепела што доводи до повећања његовог удела и до његове значајније употребе као замене за цемент у дизајну бетона. Утицај група процесних параметрара (број обрта ротора, интензитет струје, период активације, брзина активације, капацитет млина) на факторе квалитета производа (дистрибуција величине зрна, просечна величина зрна, степен микронизације, тенденција ка агломерацији, специфична површина) је праћен и процењен помоћу Методе одзивних површина, „Standard score“ анализе и Анализе главних компонената како би се изабрао најповољнији излаз. Развијени модели су могли тачно предвидети показатеље квалитета у широком обиму процесних параметара. Израчунате r^2 вредности су биле у опсегу 0.846-0.999. Оптимални узорак пепела, који је постигао вредност SS = 0.93, је добијен применом сета параметара који одговарају ситу са отвором 120 μm.*

Микроструктурне карактеристике активираних зрна пепела су процењене уз помоћ вредости добијених из копјутерског процесирања SEM слика и анализе хистограма неправилности површина.

Кључне речи: *високо-енергетско млевење; ултра-центрифугални активатор; аналитичко моделовање; скенинг-електронска микроскопија; конструкциони композити.*